

## Stability, Water Exchange, and Anion Binding Studies on Lanthanide(III) Complexes with a Macrocyclic Ligand Based on 1,7-Diaza-12-crown-4: Extremely Fast Water Exchange on the Gd<sup>3+</sup> Complex

Zoltán Pálkás,<sup>†</sup> Adrián Roca-Sabio,<sup>‡</sup> Marta Mato-Iglesias,<sup>‡</sup> David Esteban-Gómez,<sup>‡</sup> Carlos Platas-Iglesias,<sup>\*\*‡</sup> Andrés de Blas,<sup>‡</sup> Teresa Rodríguez-Blas,<sup>‡</sup> and Éva Tóth<sup>\*\*†</sup>

<sup>†</sup>Centre de Biophysique Moléculaire, CNRS, rue Charles Sadron, 45071 Orléans, Cedex 2, France, and

<sup>‡</sup>Departamento de Química Fundamental, Universidade da Coruña, Campus da Zapateira, Alejandro de la Sota 1, 15008 A Coruña, Spain

Received June 10, 2009

The picolinate-derivative ligand based on the 1,7-diaza-12-crown-4 platform (bp12c4<sup>2-</sup>) forms stable Ln<sup>3+</sup> complexes with stability constants increasing from the early to the middle lanthanides, then being relatively constant for the rest of the series (logK<sub>LnL</sub> = 16.81(0.06), 18.82(0.01), and 18.08(0.05) for Ln = La, Gd, and Yb, respectively). The complex formation is fast, allowing for direct potentiometric titrations to assess the stability constants. In the presence of Zn<sup>2+</sup>, the dissociation of [Gd(bp12c4)]<sup>+</sup> proceeds both via proton- and metal-assisted pathways, and in this respect, this system is intermediate between DTPA-type and macrocyclic, DOTA-type chelates, for which the dissociation is predominated by metal- or proton-assisted pathways, respectively. The Cu<sup>2+</sup> exchange shows an unexpected pH dependency, with the observed rate constants decreasing with increasing proton concentration. The rate of water exchange, assessed by <sup>17</sup>O NMR, is extremely high on the [Gd(bp12c4)(H<sub>2</sub>O)<sub>9</sub>]<sup>+</sup> complex ( $k_{\text{ex}}^{298} = (2.20 \pm 0.15) \times 10^8 \text{ s}^{-1}$ ), and is in the same order of magnitude as for the Gd<sup>3+</sup> aqua ion ( $k_{\text{ex}}^{298} = 8.0 \times 10^8 \text{ s}^{-1}$ ). In aqueous solution, the [Gd(bp12c4)(H<sub>2</sub>O)<sub>9</sub>]<sup>+</sup> complex is present in hydration equilibrium between nine-coordinate, monohydrated, and ten-coordinate, bishydrated species. We attribute the fast exchange to the hydration equilibrium and to the flexible nature of the inner coordination sphere. The large negative value of the activation entropy ( $\Delta S^\ddagger = -35 \pm 8 \text{ J mol}^{-1} \text{ K}^{-1}$ ) points to an associative character for the water exchange and suggests that water exchange on the nine-coordinate, monohydrated species is predominant in the overall exchange. Relaxometric and luminescence measurements on the Gd<sup>3+</sup> and Eu<sup>3+</sup> analogues, respectively, indicate strong binding of endogenous anions such as citrate, hydrogencarbonate, or phosphate to [Ln(bp12c4)]<sup>+</sup> complexes ( $K_{\text{aff}} = 280 \pm 20 \text{ M}^{-1}$ ,  $630 \pm 50 \text{ M}^{-1}$ , and  $250 \pm 20 \text{ M}^{-1}$ , respectively). In the ternary complexes, the inner sphere water molecules are fully replaced by the corresponding anion. Anion binding is favored by the positive charge of the [Ln(bp12c4)]<sup>+</sup> complexes and the adjacent position of the two inner sphere water molecules. To obtain information about the structure of the ternary complexes, the [Gd(bp12c4)(HCO<sub>3</sub>)] and [Gd(bp12c4)(H<sub>2</sub>PO<sub>4</sub>)] systems were investigated by means of density functional theory calculations (B3LYP model). They show that anion coordination provokes an important lengthening of the distances between the donor atoms and the lanthanide ion. The coordination of phosphate induces a more important distortion of the metal coordination environment than the coordination of hydrogencarbonate, in accordance with a higher binding constant for HCO<sub>3</sub><sup>-</sup> and a more important steric demand of phosphate.

### Introduction

In the past two decades there has been a renaissance of lanthanide coordination chemistry in aqueous solution,<sup>1</sup>

\*To whom correspondence should be addressed. E-mail: eva.jakabtoth@cnrs-orleans.fr.

(1) Parker, D.; Dickens, R. S.; Puschmann, H.; Crossland, C.; Howard, J. A. K. *Chem. Rev.* 2002, 102, 1977–2010.

(2) (a) *Lanthanide Probes in Life, Chemical and Earth Sciences: Theory and Practice*; Bunzli, J.-C. G., Choppin, G. R., Eds.; Elsevier: New York, 1989. (b) Caravan, P.; Ellinson, J. J.; McMurry, T. J.; Lauffer, R. B. *Chem. Rev.* 1999, 99, 2293.

mainly promoted by the successful biomedical application of lanthanide chelates in both diagnostics<sup>2</sup> and therapy.<sup>3</sup> With around 200 million doses injected so far into patients, Gd<sup>3+</sup>-based magnetic resonance imaging contrast agents are the most widely used lanthanide complexes in medicine.<sup>4</sup> By reducing the water proton relaxation times, these paramagnetic

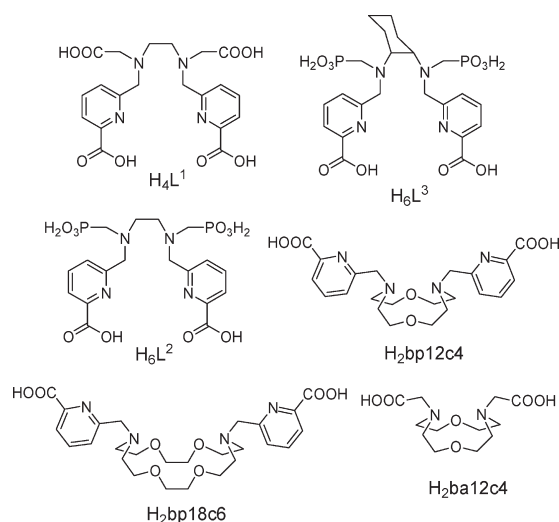
(3) (a) Liu, S. *Adv. Drug Delivery Rev.* 2008, 60, 1347–1370. (b) Roesch, F. *Radiochim. Acta* 2007, 95, 303–311. (c) Volkert, W. A.; Hoffman, T. J. *Chem. Rev.* 1999, 99, 2269–2292.

(4) *The Chemistry of Contrast Agents in Medical Magnetic Resonance Imaging*; Merbach, A. E.; Tóth, Eds.; Wiley: New York, 2001.

compounds efficiently enhance image contrast and provide an invaluable tool to delineate disease-related tissue alterations. Innovative ligand structures are continuously tested to improve the relaxation features of the  $Gd^{3+}$  complexes and to better understand the relations between chemical structure and efficacy and stability of the chelates.<sup>5,6</sup> The efficacy of these contrast agents is governed by their microscopic properties, the most important ones being the hydration number, the water exchange rate, and the rotational dynamics of the  $Gd^{3+}$  complex.<sup>7</sup> In the past years, significant efforts have been made to optimize these parameters. The main factors influencing water exchange have been identified as the steric crowding around the water binding site<sup>8</sup> and the flexibility of the inner coordination sphere.<sup>9</sup> Novel ligands ensuring optimal water exchange have been synthesized based on a rational design.<sup>10</sup> Furthermore, the stability of the chelates to be used in vivo is also a very important issue.<sup>11</sup> The complexes have to be eliminated intact from the body to avoid any toxicity associated with the release of free  $Gd^{3+}$ . Therefore, high thermodynamic stability and kinetic inertness are prerequisites for safe medical use of these chelates.<sup>12</sup>

Recently, we have reported a series of acyclic chelators bearing picolinate arms and carboxylate or phosphonate groups designed for  $Gd^{3+}$  complexation in aqueous solution (Chart 1).<sup>9,13</sup> These ligands form thermodynamically stable lanthanide complexes.<sup>14</sup> Interestingly, the water exchange rate on the phosphonate derivative  $Gd^{3+}$  complex of  $L^2$  has been found to be extremely high, comparable to that on the aqua ion itself.<sup>9</sup> This fast water exchange has been related to the flexible nature of the chelate, and indeed, the rigidification of the ligand backbone by introducing a cyclohexyl ring ( $L^3$ ) resulted in a decrease of the water exchange rate.<sup>9</sup> In a recent paper we described a novel picolinate-derivative molecule based on the 1,7-diaza-12-crown-4 platform

Chart 1



(bp12c4<sup>2-</sup>, Chart 1).<sup>15</sup> This macrocyclic chelator is expected to form kinetically more inert complexes with respect to the previous acyclic picolinate analogues, which will be an advantage to prevent toxicity. On the other hand, the optimal water exchange characteristics reported for complexes with picolinate arms could be preserved. The octadentate ligand bp12c4<sup>2-</sup> was shown to form lanthanide complexes that contain one or two inner sphere water molecules resulting in nine- and ten-coordinate chelates for the heavier and lighter lanthanides, respectively.<sup>15</sup> Complexes of lanthanides around the middle of the series are present in the form of hydration equilibrium between mono- and bis-aqua species, as it was proved by luminescence lifetime and UV-vis absorbance measurements on the  $Eu^{3+}$  analogue (the average hydration number on the  $Eu^{3+}$  complex is  $q_{ave} = 1.4$  at 298 K). While hydration equilibria are relatively common for  $Eu^{3+}$  and  $Gd^{3+}$  complexes, they usually involve eight- and nine-coordinate species.<sup>16</sup> Indeed, coordination number 10 is rather unusual in the solution chemistry of lanthanide complexes with amino-carboxylates and related ligands.<sup>17</sup> To the best of our knowledge, no water exchange data are available on ten-coordinate  $Gd^{3+}$  complexes.

Here we report the protonation constants of bp12c4<sup>2-</sup> and the thermodynamic stability constants determined for complexes with a series of lanthanides and some biologically relevant divalent metal ions. The kinetic inertness of the  $Ce^{3+}$  and  $Gd^{3+}$  complexes has been assessed in strongly acidic solutions, as well as at pH 4.5–5.5 by transmetalation studies. A variable temperature <sup>17</sup>O NMR study performed on  $[Gd(bp12c4)(H_2O)_q]^+$  yielded parameters characterizing water exchange and rotation. Finally, the formation of ternary complexes between

(5) (a) Aime, S.; Calabi, L.; Cavallotti, C.; Gianolio, E.; Giovenzana, G. B.; Losi, P.; Maiocchi, A.; Palmisano, G.; Sisti, M. *Inorg. Chem.* **2004**, *43*, 7588–7590. (b) Baranyai, Z.; Uggeri, F.; Giovenzana, G. B.; Benyei, A.; Brucher, E.; Aime, S. *Chem.—Eur. J.* **2009**, *15*, 1696–1705. (c) Gianolio, E.; Giovenzana, G. B.; Longo, D.; Longo, I.; Menegotto, I.; Aime, S. *Chem.—Eur. J.* **2007**, *13*, 5785–5797. (d) Elemento, E. M.; Parker, D.; Aime, S.; Gianolio, E.; Lattuada, L. *Org. Biomol. Chem.* **2009**, *7*, 1120–1131.

(6) Pellegatti, L.; Zhang, J.; Drahos, B.; Villette, S.; Suzenet, F.; Guillaumet, G.; Petoud, S.; Toth, E. *Chem. Commun.* **2008**, 6591–6593.

(7) Peters, J. A.; Huskens, J.; Raber, D. J. *Prog. NMR Spectrosc.* **1996**, *28*, 283–350.

(8) (a) Ruloff, R.; Toth, E.; Scopelliti, R.; Tripier, R.; Handel, H.; Merbach, A. E. *Chem. Commun.* **2002**, 2630–2631. (b) Laus, S.; Ruloff, R.; Toth, E.; Merbach, A. E. *Chem.—Eur. J.* **2003**, *9*, 3555–3566.

(9) (a) Mato-Iglesias, M.; Platas-Iglesias, C.; Djanashvili, K.; Peters, J. A.; Toth, E.; Balogh, E.; Muller, R. N.; Vander Elst, L.; de Blas, A.; Rodríguez-Blas, T. *Chem. Commun.* **2005**, 4729–4731. (b) Balogh, E.; Mato-Iglesias, M.; Platas-Iglesias, C.; Toth, E.; Djanashvili, K.; Peters, J. A.; de Blas, A.; Rodríguez-Blas, T. *Inorg. Chem.* **2006**, *45*, 8719–8728.

(10) (a) Jaszberenyi, Z.; Sour, A.; Toth, E.; Benmelouka, M.; Merbach, A. E. *Dalton Trans.* **2005**, 2713–2719. (b) Koteck, J.; Lebdusková, P.; Hermann, P.; Vander Elst, L.; Muller, R. N.; Gerales, C. F. G. C.; Maschmeyer, T.; Luke, I.; Peters, J. A. *Chem.—Eur. J.* **2003**, *9*, 5899–5915. (c) Polasek, M.; Sedinova, M.; Koteck, J.; Vander Elst, L.; Muller, R. N.; Hermann, P.; Lukes, I. *Inorg. Chem.* **2009**, *48*, 455–465.

(11) Cheng, S.; Abramova, L.; Saab, G.; Turabelidze, G.; Patel, P.; Arduino, M.; Hess, T.; Kallen, A.; Jhung, M. *JAMA* **2007**, *297*, 1542–1544.

(12) Brucher, E.; Sherry, A. D. *Stability and Toxicity of Contrast Agents. In The Chemistry of Contrast Agents in Medical Magnetic Resonance Imaging*; Tóth, E.; Merbach, A. E., Eds.; Wiley: Chichester, 2001; pp 243–279.

(13) Platas-Iglesias, C.; Mato-Iglesias, M.; Djanashvili, K.; Muller, R. N.; Vander Elst, L.; Peters, J. A.; de Blas, A.; Rodríguez-Blas, T. *Chem.—Eur. J.* **2004**, *10*, 3579–3590.

(14) Mato-Iglesias, M.; Balogh, E.; Platas-Iglesias, C.; Toth, E.; de Blas, A.; Rodríguez-Blas, T. *Dalton Trans.* **2006**, 5404–5415.

(15) Mato-Iglesias, M.; Roca-Sabio, A.; Palinkas, Z.; Esteban-Gomez, D.; Platas-Iglesias, C.; Toth, E.; de Blas, A.; Rodríguez-Blas, T. *Inorg. Chem.* **2008**, *47*, 7840–7851.

(16) (a) Graeppi, N.; Powell, D. H.; Laurenczy, G.; Zékány, L.; Merbach, A. E. *Inorg. Chim. Acta* **1995**, *235*, 311–326. (b) Platas-Iglesias, C.; Corsi, D. M.; Vander Elst, L.; Muller, R. N.; Imbert, D.; Bünzli, J.-C. G.; Tóth, É.; Maschmeyer, T.; Peters, J. A. *J. Chem. Soc., Dalton Trans.* **2003**, 727–737.

(17) (a) Valencia, L.; Martínez, J.; Macías, A.; Bastida, R.; Carvalho, R. A.; Gerales, C. F. G. C. *Inorg. Chem.* **2002**, *41*, 5300–5312. (b) Nuñez, C.; Bastida, R.; Macías, A.; Mato-Iglesias, M.; Platas-Iglesias, C.; Valencia, L. *Dalton Trans.* **2008**, 3841–3850. (c) Chatterton, N.; Bretonnière, Y.; Pecaut, J.; Mazzanti, M. *Angew. Chem., Int. Ed.* **2005**, *44*, 7595–7598.

$[\text{Gd}(\text{bp}12\text{c}4)(\text{H}_2\text{O})_q]^+$  and some biologically relevant small anions has been investigated.

## Experimental Section

The ligand has been synthesized as described in ref 15. The stock solutions of  $\text{LnCl}_3$  (Ln: La, Ce, Eu, Gd, Dy, and Yb) were made by dissolving  $\text{Ln}_2\text{O}_3$  in a slight excess of concentrated HCl in double distilled water. The excess of aqueous HCl solution was removed by evaporation. The other metal chloride solutions were made from chloride salts in double distilled water. The concentration of the solutions was determined by complexometric titration with a standardized  $\text{Na}_2\text{H}_2\text{EDTA}$  solution ( $\text{H}_4\text{EDTA}$  = ethylenediaminetetraacetic acid) using xylenol orange as indicator. Ligand stock solutions were prepared in double distilled water. The exact ligand concentration was determined from the difference in the potentiometric titration curves with KOH in the absence and in the presence of 50-fold excess of  $\text{Ca}^{2+}$ . The difference in the inflection points of the two titration curves corresponds to 2 equiv of the ligand. The  $[\text{Gd}(\text{bp}12\text{c}4)(\text{H}_2\text{O})_q]^+$  complex has been prepared by mixing equimolar quantities of a  $\text{GdCl}_3$  and ligand solution and adjusting the pH to 6.0.

**pH-Potentiometry.** Ligand protonation constants and stability constants of  $\text{Ln}^{3+}$  complexes (Ln: La, Ce, Eu, Gd, Dy and Yb) were determined by pH-potentiometric titration at 25 °C in 0.1 M KCl. The samples (3 mL) were stirred while a constant  $\text{N}_2$  flow was bubbled through the solutions. The titrations were carried out adding standardized KOH solution with a Metrohm 702 SM Titrimo automatic buret. A Metrohm 692 pH/ion-meter was used to measure pH. The  $\text{H}^+$  concentration was obtained from the measured pH values using the correction method proposed by Irving et al.<sup>18</sup> The protonation and stability constants were calculated from parallel titrations with the program PSEQUAD.<sup>19</sup> The errors given correspond to one standard deviation.

**Kinetic Studies.** The proton assisted dissociation of the  $\text{Ce}^{3+}$  complex of  $\text{bp}12\text{c}4^{2-}$  has been studied in the presence of a large excess of HCl, where the complex is unstable. The reaction was followed at 25 °C by monitoring the decrease of the absorbance of the complex at 280 nm in the range of proton concentrations 0.001–0.3 M. The concentration of the complex was 0.0001 M.

The exchange reactions between  $[\text{Gd}(\text{bp}12\text{c}4)(\text{H}_2\text{O})_q]^+$  and  $\text{Zn}^{2+}$  have been studied by measuring the longitudinal relaxation rates ( $1/T_1$ ) of water protons on a Bruker Avance 500 (11.75 T) NMR spectrometer in the pH range 4.6–5.3. The  $\text{Zn}^{2+}$  concentration varied between 0.005 and 0.03 M, while the concentration of the  $\text{Gd}^{3+}$  complex was 0.0002 M. 0.02 M *N*-methyl-piperazine was used as buffer, and the ionic strength was 0.1 M KCl. The relaxivities,  $r_1$ , were calculated from the measured  $1/T_{1\text{obs}}$  water proton relaxation rates according to eq 1, where  $1/T_{1\text{w}}$  is the relaxation rate of water at the given temperature, and  $[\text{Gd}]$  is the  $\text{Gd}^{3+}$  concentration in mM.

$$\frac{1}{T_{1\text{obs}}} = \frac{1}{T_{1\text{w}}} + \frac{1}{T_{1\text{p}}} = \frac{1}{T_{1\text{w}}} + r_1 \times [\text{Gd}] \quad (1)$$

The pseudo-first-order rate constants ( $k_{\text{obs}}$ ) were calculated by fitting the relaxation rate data to eq 2,

$$r_{1t} = (r_{10} - r_{1e}) \exp(-k_{\text{obs}}t) + r_{1e} \quad (2)$$

where  $r_{1t}$ ,  $r_{10}$ , and  $r_{1e}$  are the relaxivity values at time  $t$ , time zero, and at equilibrium, respectively.

The dissociation rate constants of the metal exchange reaction with  $\text{Cu}^{2+}$  were determined by UV–vis measurements following the increase of the absorbance at 300 nm. The

concentration of the gadolinium(III)-complex was 0.0001 M, the  $\text{Cu}^{2+}$  concentration varied between 0.001 and 0.02 M, and MES was used as buffer. The rate of the exchange reaction was studied at different pHs (4.6–5.3). The least-squares fit of the kinetic data was performed by using Micromath Scientist version 2.0 (Salt Lake City, UT, U.S.A.). The reported errors correspond to one standard deviation obtained by the statistical analysis.

**$^{17}\text{O}$  NMR Measurements.** The transverse and longitudinal  $^{17}\text{O}$  relaxation rates ( $1/T_{1,2}$ ) and the chemical shifts were measured in a  $[\text{Gd}(\text{bp}12\text{c}4)(\text{H}_2\text{O})_q]^+$  aqueous solution in the temperature range 280–345 K, on a Bruker Avance 500 (11.75 T, 67.8 MHz) spectrometer. The temperature was calculated according to previous calibration with ethylene glycol and methanol.<sup>20</sup> An acidified water solution was used as reference ( $\text{HClO}_4$ , pH 3.3). Longitudinal  $^{17}\text{O}$  relaxation times ( $T_1$ ) were measured by the inversion–recovery pulse sequence,<sup>21</sup> and the transverse relaxation times ( $T_2$ ) were obtained by the Carr–Purcell–Meiboom–Gill spin–echo technique.<sup>22</sup> The technique of the  $^{17}\text{O}$  NMR measurements on  $\text{Gd}^{3+}$  complexes have been described elsewhere.<sup>23</sup> The samples were sealed in glass spheres fitted into 10 mm NMR tubes, to eliminate susceptibility corrections to the chemical shifts.<sup>24</sup> To improve sensitivity in  $^{17}\text{O}$  NMR,  $^{17}\text{O}$ -enriched water (10%  $\text{H}_2^{17}\text{O}$ , CortecNet) was added to the solutions to yield around 1%  $^{17}\text{O}$  enrichment. The molal concentration of the  $[\text{Gd}(\text{bp}12\text{c}4)(\text{H}_2\text{O})_q]^+$  complex in the sample used for  $^{17}\text{O}$  NMR was 0.0263 mol/kg (pH 6.0). The  $^{17}\text{O}$  NMR data have been evaluated according to the Solomon–Bloembergen–Morgan theory of paramagnetic relaxation,<sup>25</sup> though using a simplified exponential model for the temperature dependency of the electron spin relaxation rate (see Supporting Information). The least-squares fit of the  $^{17}\text{O}$  NMR data was performed by using Micromath Scientist version 2.0 (Salt Lake City, UT, U.S.A.). The reported errors correspond to one standard deviation obtained by the statistical analysis.

**Ternary Complex Formation.** The formation of ternary complexes between  $[\text{Gd}(\text{bp}12\text{c}4)(\text{H}_2\text{O})_q]^+$  and carbonate, phosphate, and citrate ions has been studied by measuring the longitudinal relaxation rates ( $1/T_1$ ) of water protons on a Bruker NMR spectrometer at 500 MHz and 25 °C. The concentration of the  $\text{Gd}^{3+}$  complex was 1 mM while the concentration of each anion varied between 0 and 36 mM by adding 15  $\mu\text{L}$  portions of the anion stock solution to 0.5 mL of complex solution in the NMR tube. The exact concentration of the complex and the anions were calculated at each point; 0.01 M HEPES was used as buffer to maintain a constant pH (pH = 7.4), while the ionic strength was 0.15 M NaCl.

Excitation and emission spectra were recorded on a Perkin-Elmer LS-50B spectrometer. Luminescence lifetimes were calculated from the monoexponential fitting of the average decay data, and they are averages of at least 3–5 independent determinations. Anion binding studies were performed by using the same instrument on about  $10^{-5}$  M solutions of the  $[\text{Eu}(\text{bp}12\text{c}4)(\text{H}_2\text{O})_q]^+$  complex at 25 °C. Typically, aliquots of a fresh standard  $10^{-5}$  M solution of the  $\text{Eu}^{3+}$  complex containing the anion (up to 0.01 M) were used, and the emission spectra of the samples were recorded. The pH of the solutions was adjusted to  $7.4 \pm 0.05$  by using HEPES buffer (0.01 M), and the ionic strength was 0.15 M NaCl.

(20) Raiford, D. S.; Fisk, C. L.; Becker, E. D. *Anal. Chem.* **1979**, *51*, 2050–2051.

(21) Vold, R. L.; Waugh, J. S.; Klein, M. P.; Phelps, D. E. *J. Chem. Phys.* **1968**, *48*, 3831–3832.

(22) Meiboom, S.; Gill, D. *Rev. Sci. Instrum.* **1958**, *29*, 688–691.

(23) Micskei, K.; Helm, L.; Brücher, E.; Merbach, A. E. *Inorg. Chem.* **1993**, *18*, 3844.

(24) Hugi, A. D.; Helm, L.; Merbach, A. E. *Helv. Chim. Acta* **1985**, *68*, 508–521.

(25) Tóth, É.; Helm, L.; Merbach, A. E. Relaxivity of Gadolinium(III) Complexes: Theory and Mechanism. In *The Chemistry of Contrast Agents in Medical Magnetic Resonance Imaging*; Merbach, A. E., Tóth, É., Eds.; Wiley: New York, 2001; Chapter 2, p 45–120.

(18) Irving, H. M.; Miles, M. G.; Pettit, L. *Anal. Chim. Acta* **1967**, *28*, 475–488.

(19) Zékány L.; Nagypál, I. In *Computation Methods for Determination of Formation Constants*; Leggett, D. J., Ed.; Plenum: New York, 1985; p 291.

**Computational Details.** All calculations were performed employing hybrid density functional theory (DFT) with the B3LYP exchange-correlation functional,<sup>26,27</sup> and the Gaussian 03 package (Revision C.01).<sup>28</sup> Full geometry optimizations of the  $[\text{Gd}(\text{bp}12\text{c}4)]^+ \cdot \text{HCO}_3^-$ ,  $[\text{Gd}(\text{bp}12\text{c}4)]^+ \cdot \text{H}_2\text{PO}_4^-$ , and  $[\text{Gd}(\text{bp}12\text{c}4)]^+ \cdot \text{HPO}_4^{2-}$  systems were performed in vacuo by using the effective core potential (ECP) of Dolg et al. and the related [5s4p3d]-GTO valence basis set for Gd,<sup>29</sup> and the 6-31G(d) basis set for C, H, N, O, and P atoms. The stationary points found on the potential energy surfaces as a result of the geometry optimizations have been tested to represent energy minima rather than saddle points via frequency analysis.

## Results and Discussion

**Ligand Protonation Constants and Stability Constants of the Complexes.** The protonation constants of  $\text{bp}12\text{c}4^{2-}$  as well as the stability constants of its metal complexes formed with  $\text{Ln}^{3+}$  and biologically relevant divalent ions were determined by potentiometric titrations; the constants and standard deviations are given in Table 1, which also lists those of  $\text{bp}18\text{c}6^{2-}$  (Chart 1).<sup>32</sup> The ligand protonation constants are defined as in eq 3, and the stability and protonation constants of the metal chelates are expressed in eqs 4 and 5, respectively. The titration curves of the lanthanide complexes all show a deprotonation step at high pH (> 8) indicating the formation of a monohydroxo complex (Figure 1). The formation of these monohydroxo complexes has been characterized by the protonation constant  $K_{\text{MLOH}}$ , as defined in eq 6.

$$K_i = \frac{[\text{H}_i\text{L}]}{[\text{H}_{i-1}\text{L}][\text{H}^+]} \quad (3)$$

$$K_{\text{ML}} = \frac{[\text{ML}]}{[\text{M}][\text{L}]} \quad (4)$$

$$K_{\text{MHL}} = \frac{[\text{MHL}]}{[\text{ML}][\text{H}^+]} \quad (5)$$

$$K_{\text{MLOH}} = \frac{[\text{ML}]}{[\text{ML}(\text{OH})][\text{H}^+]} \quad (6)$$

Four protonation constants could be determined for the  $\text{bp}12\text{c}4^{2-}$  ligand. The first two  $\log K$  values correspond

(26) Becke, A. D. *J. Chem. Phys.* **1993**, *98*, 5648–5652.

(27) Lee, C.; Yang, W.; Parr, R. G. *Phys. Rev. B* **1988**, *37*, 785–789.

(28) Frisch, M. J.; Trucks, G. W.; Schlegel, H. B.; Scuseria, G. E.; Robb, M. A.; Cheeseman, J. R.; Montgomery, Jr., J. A.; Vreven, T.; Kudin, K. N.; Burant, J. C.; Millam, J. M.; Iyengar, S. S.; Tomasi, J.; Barone, V.; Mennucci, B.; Cossi, M.; Scalmani, G.; Rega, N.; Petersson, G. A.; Nakatsuji, H.; Hada, M.; Ehara, M.; Toyota, K.; Fukuda, R.; Hasegawa, J.; Ishida, M.; Nakajima, T.; Honda, Y.; Kitao, O.; Nakai, H.; Klene, M.; Li, X.; Knox, J. E.; Hratchian, H. P.; Cross, J. B.; Adamo, C.; Jaramillo, J.; Gomperts, R.; Stratmann, R. E.; Yazyev, O.; Austin, A. J.; Cammi, R.; Pomelli, C.; Ochterski, J. W.; Ayala, P. Y.; Morokuma, K.; Voth, G. A.; Salvador, P.; Dannenberg, J. J.; Zakrzewski, V. G.; Dapprich, S.; Daniels, A. D.; Strain, M. C.; Farkas, O.; Malick, D. K.; Rabuck, A. D.; Raghavachari, K.; Foresman, J. B.; Ortiz, J. V.; Cui, Q.; Baboul, A. G.; Clifford, S.; Cioslowski, J.; Stefanov, B. B.; Liu, G.; Liashenko, A.; Piskorz, P.; Komaromi, I.; Martin, R. L.; Fox, D. J.; Keith, T.; Al-Laham, M. A.; Peng, C. Y.; Nanayakkara, A.; Challacombe, M.; Gill, P. M. W.; Johnson, B.; Chen, W.; Wong, M. W.; Gonzalez, C.; Pople, J. A. *Gaussian 03*; Gaussian, Inc.: Wallingford, CT, 2004.

(29) Dolg, M.; Stoll, H.; Savin, A.; Preuss, H. *Theor. Chim. Acta* **1989**, *75*, 173–194.

**Table 1.** Protonation Constants of  $\text{bp}12\text{c}4^{2-}$  and Related Ligands and Stability Constants of Their  $\text{Ln}^{3+}$  and  $\text{M}^{2+}$  Complexes (25 °C;  $I = 0.1 \text{ M}$  (KCl))

	$\text{bp}12\text{c}4^{2-}$	$\text{bp}18\text{c}6^a$	$\text{ba}12\text{c}4^b$	EDTA <sup>c</sup>	DTPA <sup>d</sup>
$\log K_1$	9.16 (0.03)	7.41	9.53	10.17	10.34
$\log K_2$	7.54 (0.04)	6.85	7.46	6.11	8.59
$\log K_3$	3.76 (0.05)	3.32	2.11	2.68	4.25
$\log K_4$	2.79 (0.04)	2.36			2.71
$\log K_{\text{LaL}}$	16.81 (0.06)	14.99		15.46	18.23
$\log K_{\text{LaLOH}}$	10.87 (0.08)				
$\log K_{\text{CeL}}$	16.94 (0.09)	15.11		15.94	19.09
$\log K_{\text{CeLOH}}$	9.78 (0.07)				
$\log K_{\text{EuL}}$	18.62 (0.08)	13.01		17.32	20.87
$\log K_{\text{EuLOH}}$	9.96 (0.07)				
$\log K_{\text{GdL}}$	18.82 (0.01)	13.02		17.35	20.73
$\log K_{\text{GdLOH}}$	9.49 (0.03)				
$\log K_{\text{DyL}}$	18.11 (0.08)	11.72		18.28	21.11
$\log K_{\text{DyLOH}}$	10.0(0.1)				
$\log K_{\text{YbL}}$	18.08 (0.05)	8.89		19.48	22.59
$\log K_{\text{YbLOH}}$	10.15 (0.08)				
$\log K_{\text{CaL}}$	12.09 (0.06)		8.50	10.8	10.7
$\log K_{\text{ZnL}}$	18.12 (0.03)		12.28	16.5	18.29
$\log K_{\text{CuL}}$	19.56 (0.04)		15.95	18.8	21.5
$\log K_{\text{CuHL}}$	6.52 (0.09)				4.8

<sup>a</sup> Ref 32. <sup>b</sup> Ref 33.  $I = 0.1 \text{ M Me}_4\text{NNO}_3$ . <sup>c</sup> Ref 34. <sup>d</sup> Ref 34b.

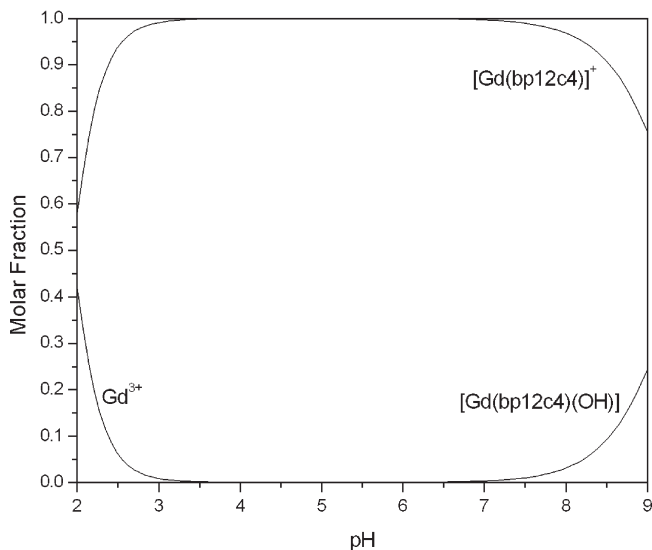
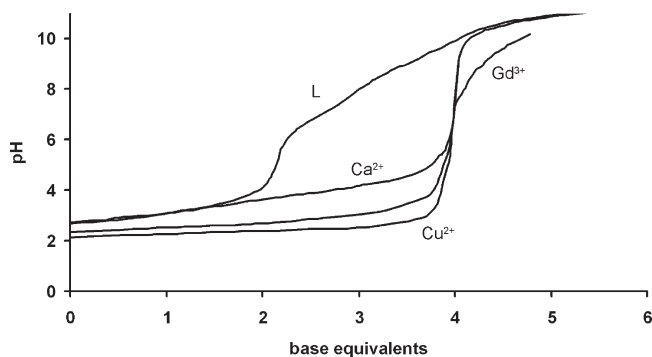


**Figure 1.** Top: Potentiometric pH titration curves for the ligand  $\text{bp}12\text{c}4^{2-}$  in the absence and in the presence of some of the metal ions studied at 1:1 metal to ligand ratio. Bottom: Species distribution of the  $[\text{Gd}(\text{bp}12\text{c}4)]$  system at 1:1 Gd:bp12c4 ratio,  $[\text{Gd}^{3+}] = 1 \text{ mM}$  [ $I = 0.1 \text{ M}$  KCl, 25 °C].

to the protonation of the macrocyclic nitrogens.  $\log K_1$  is somewhat lower for  $\text{bp12c4}^{2-}$  than for the bisacetate derivative of the same macrocycle ( $\text{ba12c4}$ , Chart 1). It is in accordance with previous observations where a diminution of the amine basicity, though more important than here, has been observed on replacement of the acetate arm by 6-methyl-2-pyridinecarboxylate groups.<sup>30</sup> The third and fourth protonation steps of  $\text{bp12c4}^{2-}$  are likely associated to the carboxylic acid groups.<sup>30,31</sup>

The stability constants of the lanthanide complexes of  $\text{bp12c4}^{2-}$  could be obtained from direct potentiometric titrations, as the complex formation was fast. The complex stability increases from the early lanthanides to the middle of the series, then remains relatively constant or slightly declines for the heavier lanthanides. In this respect, this chelator is similar to DTPA, in contrast to most of the poly(amino carboxylate) ligands, such as EDTA, which form complexes of increasing stability all across the lanthanide series because of the increase of charge density on the metal ions. As expected, the peculiar selectivity for the light lanthanides of the eighteen-membered macrocyclic ligand  $\text{bp18c6}^{2-32}$  is not observed for  $\text{bp12c4}^{2-}$ . Given its much smaller size, this twelve-membered macrocycle provides an optimal fit for smaller lanthanides. For the first half of the lanthanide series ( $\text{Ln} = \text{La} - \text{Gd}$ ), the stability constants fall in between those reported for EDTA and DTPA complexes. For the heaviest lanthanides, the stability constants are somewhat lower for  $\text{bp12c4}^{2-}$  complexes than for EDTA ones. We should note the high stabilities of  $\text{Cu}^{2+}$ ,  $\text{Zn}^{2+}$ , and  $\text{Ca}^{2+}$  complexes formed with  $\text{bp12c4}^{2-}$  with respect to those for the bis(acetate) analogue  $\text{ba12c4}$ .<sup>33</sup>

At high pH, all lanthanide complexes undergo deprotonation, likely occurring on the coordinated water molecule, to form monohydroxo complexes.<sup>35</sup> The  $K_{\text{MLOH}}$  constants characterizing this deprotonation step decrease from the beginning to the middle of the series to reach the lowest value for  $[\text{Gd}(\text{bp12c4})(\text{OH})]$ , then again slightly increase for the heavier lanthanides. The trend observed in the first part of the series can be easily rationalized by the increasing charge density of the metal ions. The increase observed toward the end of the series could be related to a diminution in the hydration from two to one for the small lanthanides. The species distribution

diagram obtained for the representative  $\text{Gd}^{3+}$  complex is depicted in Figure 1.

To better compare the stability of  $\text{Gd}(\text{bp12c4})^+$  to other  $\text{Gd}^{3+}$  complexes, we have calculated the pGd value at pH 7.4,  $c_{\text{L}} = 1 \times 10^{-5}$  M and  $c_{\text{Gd}} = 1 \times 10^{-6}$  M ( $\text{pGd} = -\log[\text{Gd}^{3+}]_{\text{free}}$ ). pGd values reflect the influence of the ligand basicity and the protonation of the complex on the stability; the higher the pGd, the more stable is the complex under the given conditions. For  $\text{Gd}(\text{bp12c4})^+$  we obtain  $\text{pGd} = 17.6$ , a slightly lower value than that calculated for  $\text{GdDTPA}$  ( $\text{pGd} = 19.1$ ), which clearly shows the good complexing ability of our ligand toward lanthanides.

**Kinetic Studies on  $[\text{Ln}(\text{bp12c4})(\text{H}_2\text{O})_q]^+$  Complexes.** It has been recognized early on that the fate of the  $\text{Gd}^{3+}$  complexes in vivo cannot be predicted on the basis of equilibrium considerations.<sup>12,36</sup> The kinetic inertness of the complexes plays a crucial role in determining the  $\text{Gd}^{3+}$  release in vivo. The kinetic stability can be characterized by rate constants of exchange reactions that might take place in the plasma. Among those, the most important is probably the displacement of  $\text{Gd}^{3+}$  by the endogenously abundant  $\text{Cu}^{2+}$  and  $\text{Zn}^{2+}$  ions. Since the dissociation of the complexes and the metal exchange reactions are relatively slow processes around physiological pH, the dissociation of many complexes has been studied in acidic solutions.<sup>12,36</sup> More recently, detailed kinetic studies have been conducted at higher pHs (3.5–6) to investigate the role of transmetalation with  $\text{Zn}^{2+}$  and  $\text{Cu}^{2+}$ .<sup>37</sup> In general terms, linear DTPA-type  $\text{Gd}^{3+}$  chelates are kinetically much less inert than the macrocyclic, DOTA-type complexes. At physiological pH, the dissociation of linear chelates proceeds mainly via transmetalation, which largely takes over the acid-assisted pathway. The reaction rates of the metal exchange between  $\text{GdDTPA}$  and  $\text{Cu}^{2+}$  or  $\text{Zn}^{2+}$  are independent of pH above pH 4.5, indicating that the exchange predominantly occurs via direct attack of these metals on the  $\text{Gd}^{3+}$  complex.<sup>37</sup> In contrast, the dissociation of macrocyclic chelates is much slower and independent of the exchanging metal ion concentration, showing that it occurs through proton-assisted pathways.<sup>38–40</sup>

We have assessed the kinetic inertness of the  $[\text{Ln}(\text{bp12c4})]^+$  complexes by following the acid-assisted dissociation in strongly acidic solutions for the  $\text{Ce}^{3+}$  complex, and the transmetalation with  $\text{Zn}^{2+}$  and  $\text{Cu}^{2+}$  at pH 4.5–5.5 for the  $\text{Gd}^{3+}$  analogue. In the presence of a large excess of acid (0.001–0.3 M HCl), the complex is thermodynamically unstable. The reaction was followed for the  $\text{Ce}^{3+}$  complex by monitoring the decrease of the absorbance of the complex at 280 nm. The observed first order dissociation rate constants follow a quadratic dependence on the proton concentration (eq 7) showing

(30) Chatterton, N.; Gateau, C.; Mazzanti, M.; Pecaut, J.; Borel, A.; Helm, L.; Merbach, A. *Dalton Trans.* **2005**, 1129–1135.

(31) (a) Ferreiros-Martinez, R.; Esteban-Gomez, D.; Platas-Iglesias, C.; de Blas, A.; Rodriguez-Blas, T. *Dalton Trans.* **2008**, 5754–5765. (b) Pellissier, A.; Bretonniere, Y.; Chatterton, N.; Pecaut, J.; Delangle, P.; Mazzanti, M. *Inorg. Chem.* **2007**, *46*, 3714–3725.

(32) Roca Sabio, A.; Mato-Iglesias, M.; Esteban-Gomez, D.; Toth, E.; de Blas, A.; Platas-Iglesias, C.; Rodriguez-Blas, T. *J. Am. Chem. Soc.* **2009**, *131*, 3331–3341.

(33) Amorim, M. T. S.; Delgado, R.; Frausto da Silva, J. J. R. *Polyhedron* **1992**, *11*, 1891–1899.

(34) (a) Lacoste, R. G.; Christoffers, G. V.; Martell, A. E. *J. Am. Chem. Soc.* **1965**, *87*, 2385–2388. (b) Martell, A. E.; Motekaitis, R. J.; Smith, R. M. *NIST Critically selected stability constants of metal complexes database*, Version 8.0 for windows; National Institute of Standards and Technology: Gaithersburg, MD, 2004; Standard Reference Data Program.

(35) Nonat, A.; Fries, P. H.; Pecaut, J.; Mazzanti, M. *Chem.—Eur. J.* **2007**, *13*, 8489–8506.

(36) Brücher, E. In *Contrast Agents I. Magnetic Resonance Imaging*; Krause, W., Ed.; Springer Verlag: Berlin, 2002; Topics in Current Chemistry, Vol. 221, p 104.

(37) Sarka, L.; Burai, L.; Brucher, E. *Chem.—Eur. J.* **2000**, *6*, 719–724.

(38) Tóth, E.; Brücher, E.; Lazar, I.; Toth, I. *Inorg. Chem.* **1994**, *33*, 4070–4076.

(39) Balogh, E.; Tripier, R.; Ruloff, R.; Toth, E. *Dalton Trans.* **2005**, 1058–1065.

(40) Brucher, E.; Sherry, A. D. *Inorg. Chem.* **1990**, *29*, 1555–1559.

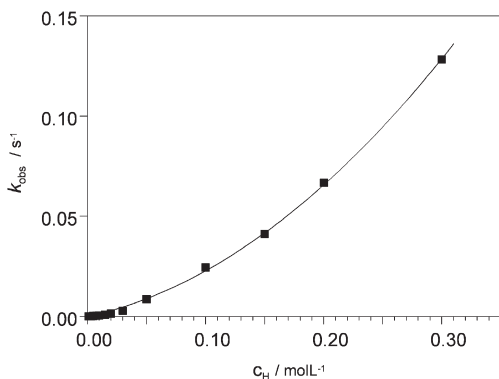


**Figure 2.** Pseudo-first-order rate constants,  $k_{\text{obs}}$ , as a function of the proton concentration in the dissociation of  $[\text{Ce}(\text{bp}12\text{c}4)]^+$  (0.0001 M;  $I = 0.1$  M KCl).

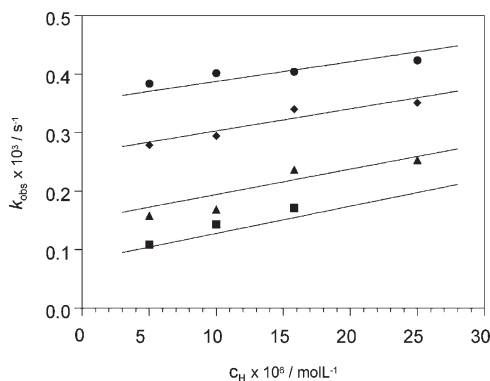


**Figure 3.** Plots of  $k_{\text{obs}}$  versus hydrogen ion concentration for the reaction between  $[\text{Gd}(\text{bp}12\text{c}4)]^+$  and  $\text{Zn}^{2+}$ .  $c_{\text{Zn}} = 5$  mM (■), 10 mM (▲), 20 mM (◆) and 30 mM (●).

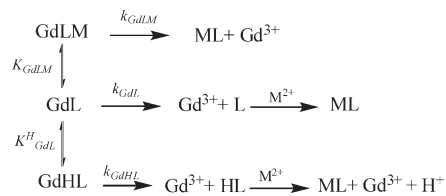
the role of proton-catalyzed pathways in the dissociation (Figure 2).

$$k_{\text{obs}} = k_0 + k' \times [\text{H}^+] + k'' \times [\text{H}^+]^2 \quad (7)$$

Similar behavior was reported for the dissociation of various acyclic  $\text{Ln}^{3+}$  complexes, including DTPA and pyridine-aminocarboxylate ligands.<sup>6,41,42</sup> It indicates that the dissociation might take place by proton-independent (characterized by  $k_0$ ) and proton-assisted pathways, presumably with the formation and dissociation of mono- and diprotonated complexes (characterized by  $k'$  and  $k''$ , respectively). The constants fitted are  $k' = 0.143 \pm 0.009 \text{ M}^{-1} \text{ s}^{-1}$  and  $k'' = 0.96 \pm 0.03 \text{ M}^{-2} \text{ s}^{-1}$ , while  $k_0$  had to be fixed to 0. When fitting  $k_0$ , we obtained a small negative value with a large error. This is not surprising since in such strongly acidic solutions the dissociation pathways involving protonated complexes are much more important than the spontaneous dissociation.

In the exchange reaction between  $\text{Gd}(\text{bp}12\text{c}4)^+$  and  $\text{Zn}^{2+}$ , the observed pseudo-first order rate constants depend on both the proton and the  $\text{Zn}^{2+}$  concentration (pH 4.6–5.3; Figure 3). They increase by increasing proton and metal ion concentration, indicating that both proton- and metal-assisted pathways play a role. In this

**Scheme 1.** Possible Reaction Pathways for the Dissociation of  $[\text{Gd}(\text{bp}12\text{c}4)]^+$  in the Presence of a Divalent Metal Ion  $\text{M}^{2+}$



respect, this system is intermediate between DTPA-type and macrocyclic chelates, for which the dissociation is predominated by metal- or proton-assisted pathways, respectively. Taking into account previous studies<sup>37</sup> and the pH- and Zn-dependency of the  $k_{\text{obs}}$  values (Figure 3), the following possible reaction pathways are assumed (Scheme 1):

According to this reaction scheme, the rate of the exchange reaction can be given as in eq 8:

$$-\frac{d[\text{GdL}]_t}{dt} = k_{\text{GdL}}[\text{GdL}] + k_{\text{GdHL}}[\text{GdHL}] + k_{\text{GdLM}}[\text{GdLM}] \quad (8)$$

In eq 8 the first term refers to the spontaneous dissociation of the complex, the second to the proton-assisted dissociation, while the last contribution describes the metal-assisted dissociation. The equilibrium constants for the protonated and the dinuclear species are given by eqs 5 and 9, respectively:

$$K_{\text{GdLM}} = \frac{[\text{GdLM}]}{[\text{GdL}][\text{M}]} \quad (9)$$

The following expression can be derived for the pseudo-first-order rate constant of the dissociation:

$$k_{\text{obs}} = \frac{k_0 + k_1[\text{H}^+] + k_{\text{M}}[\text{M}]}{1 + K_{\text{HGdL}}[\text{H}^+] + K_{\text{GdLM}}[\text{M}]} \quad (10)$$

with  $k_0 = k_{\text{GdL}}$ ,  $k_1 = k_{\text{GdHL}} \times K_{\text{HGdL}}$ , and  $k_{\text{M}} = k_{\text{GdLM}} \times K_{\text{GdLM}}$ . In the potentiometric study, we could not identify any protonated complex at pH > 1.8, which means that if there is any, its protonation constant  $\log K_{\text{HGdL}}$  has to be very low. The pseudo-first-order rate constants of the exchange reaction between  $[\text{Gd}(\text{bp}12\text{c}4)]^+$  and  $\text{Zn}^{2+}$  shown in Figure 3 were fitted to eq 10. During the fitting procedure  $k_0$  was fixed at zero, otherwise small negative values with a large error would be obtained. The rate constants  $k_1$  and  $k_{\text{M}}$ , as well as the protonation constant  $K_{\text{HGdL}}$  and the stability constant of the dinuclear complex,  $K_{\text{GdLZn}}$ , were calculated; they are listed and compared to those for  $\text{GdDTPA}^{2-}$  in Table 2.

The observed rate constants for the metal-exchange reaction between  $[\text{Gd}(\text{bp}12\text{c}4)]^+$  and  $\text{Cu}^{2+}$  also depend on both the proton and the  $\text{Cu}^{2+}$  concentration; however, their proton dependency shows an unexpected trend (Figure 4). In contrast to previously reported complexes and to the exchange between  $[\text{Gd}(\text{bp}12\text{c}4)]^+$  and  $\text{Zn}^{2+}$ , here the rate constants decrease with increasing proton concentration indicating an unusual reaction pathway. The pH dependency is more important when the  $\text{Cu}^{2+}$  is

(41) Brücher, E.; Laurency, G. *J. Inorg. Nucl. Chem.* **1981**, *43*, 2089–2096.

(42) Jakab, S.; Kovacs, Z.; Burai, L.; Brücher, E. *Magy. Kém. Foly.* **1993**, *99*, 391–396.

**Table 2.** Rate Constants Obtained for the Exchange Reaction of [Gd(bp12c4)]<sup>+</sup> with Zn<sup>2+</sup> and Cu<sup>2+</sup> at 25 °C

	[Gd(bp12c4)] <sup>+</sup>		[Gd(DTPA)] <sup>2-</sup> <sup>a</sup>	
	Zn <sup>2+</sup> exchange	Cu <sup>2+</sup> exchange	Zn <sup>2+</sup> exchange	Cu <sup>2+</sup> exchange
$k_1/\text{M}^{-1}\text{s}^{-1}$	$5.0 \pm 1.0$	<sup>b</sup>	$0.58^c$	
$k_M/\text{M}^{-1}\text{s}^{-1}$	$0.018 \pm 0.006$	$0.047 \pm 0.010$	$0.056$	$0.93$
$K_{\text{GdLM}}/\text{M}^{-1}$	$16 \pm 10$	$10 \pm 7$	$7$	$13$
$\log K_{\text{HGdL}}$	$1.6 \pm 0.6$	$1.6^d$	$2.0$	
$k_{\text{OH}}/\text{M}^{-2}\text{s}^{-1}$		$(2 \pm 0.9) \times 10^8$		

<sup>a</sup> Ref 37. <sup>b</sup> Set to zero during the fitting procedure (see text). <sup>c</sup> From Eu<sup>3+</sup> exchange. <sup>d</sup> Fixed in the fit.

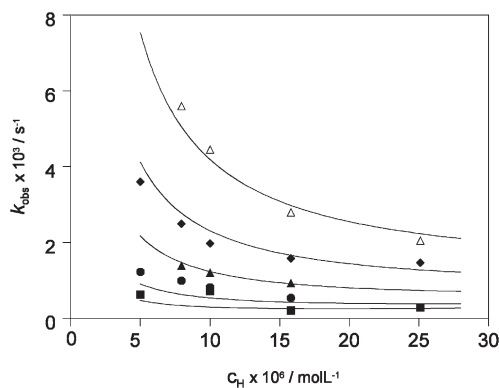


**Figure 4.** Plots of  $k_{\text{obs}}$  versus hydrogen ion concentration for the reaction between [Gd(bp12c4)]<sup>+</sup> and Cu<sup>2+</sup>.  $C_{\text{Cu}} = 1 \text{ mM}$  (■),  $2 \text{ mM}$  (●),  $5 \text{ mM}$  (▲),  $10 \text{ mM}$  (◆), and  $20 \text{ mM}$  (△).

in high concentration, while at lower copper concentration the  $k_{\text{obs}}$  values remain almost constant with pH, as it has been observed for the metal exchange of various DTPA-type Ln<sup>3+</sup> complexes. This phenomenon could be explained by the formation of a protonated H[Gd-(bp12c4)]<sup>2+</sup> complex that dissociates slower than the dinuclear Cu-[Gd(bp12c4)]<sup>3+</sup> complex transitionally formed by the direct attack of the exchanging metal ion. However, a protonated complex could not be identified in the potentiometric titration, which can be rationalized by the positive charge of [Gd(bp12c4)]<sup>+</sup>, unfavorable for protonation. An attempt to fit the  $k_{\text{obs}}$  data to eq 10 resulted in the following values:  $k_1 = 10 \text{ M}^{-1}\text{s}^{-1}$ ,  $k_M = 1.2 \text{ M}^{-1}\text{s}^{-1}$ ,  $K_{\text{GdLCu}} = 11$ , and  $\log K_{\text{HGdL}} = 5.6$ . While all the other parameters have reasonable values, the value of  $\log K_{\text{HGdL}} = 5.6$  is inconceivable, since such high protonation constant should be well detectable on the pH-potentiometric titration curve, and therefore this model cannot account for the unprecedented pH dependency of the rate constants observed for the Cu<sup>2+</sup> transmetalation. In another hypothesis, the transitionally formed dinuclear Cu-[Gd(bp12c4)]<sup>3+</sup> species would dissociate via a hydroxide-assisted pathway which is faster than the proton-assisted dissociation of the [Gd(bp12c4)]<sup>+</sup> complex itself. This hypothesis is based on the three positive charges of the dinuclear species which makes it more prone to an eventual hydroxide-catalyzed dissociation. The lanthanide complexes of bp12c4<sup>2-</sup> all have shown a tendency to form monohydroxo complexes in the potentiometric study. On the other hand, Cu<sup>2+</sup> is known to form hydroxo-complexes at lower pH than Zn<sup>2+</sup>, which could explain the different behavior of the two metals. To take into account such a pathway, we can

include a term  $k_{\text{OH}} \times [\text{Cu}^{2+}] \times [\text{OH}^-]$  in the numerator of the expression of  $k_{\text{obs}}$  to give eq 11:

$$k_{\text{obs}} = \frac{k_0 + k_1[\text{H}^+] + k_M[\text{M}] + k_{\text{OH}}[\text{M}][\text{OH}^-]}{1 + K_{\text{HGdL}}[\text{H}^+] + K_{\text{GdLM}}[\text{M}]} \quad (11)$$

The fit of the experimental data to this equation is shown in Figure 4, and the fitted parameters are reported in Table 2. We do not have proofs that a hydroxide-assisted dissociation is responsible for the unprecedented pH dependence of the Cu<sup>2+</sup>-exchange kinetics observed for [Gd(bp12c4)]<sup>+</sup>, but the data for the Cu<sup>2+</sup> exchange represent a tentative explanation of the experimental evidence. It is to be mentioned, however, that Margerum et al. reported a greater kinetic activity for Cu(OH)<sup>+</sup> in substitution reactions than for Cu<sup>2+</sup>.<sup>43</sup>

In comparison to GdDTPA<sup>2-</sup>, the proton-assisted dissociation is more rapid, while the zinc- or copper-assisted transmetalation is less efficient for [Gd(bp12c4)]<sup>+</sup>. If we consider that at physiological pH the acid-catalyzed pathway becomes negligible, the [Gd(bp12c4)]<sup>+</sup> complex is more resistant to dissociation than its DTPA analogue. In overall, however, the kinetic inertness of [Gd(bp12c4)]<sup>+</sup> is not considerably higher than that of GdDTPA<sup>2-</sup>.

**<sup>17</sup>O NMR Measurements and Water Exchange on [Gd(bp12c4)(H<sub>2</sub>O)<sub>q</sub>]<sup>+</sup>.** To assess parameters characterizing the water exchange and rotational dynamics on [Gd-(bp12c4)(H<sub>2</sub>O)<sub>q</sub>]<sup>+</sup>, we have measured variable temperature transverse and longitudinal <sup>17</sup>O NMR relaxation rates and chemical shifts at 11.7 T. Previous luminescence and high resolution UV-vis absorbance data obtained on the corresponding Eu<sup>3+</sup> analogue proved the existence of a hydration equilibrium, with an average hydration number of  $q_{\text{av}} = 1.4$  at 298 K.<sup>15</sup> The temperature dependence of the hydration equilibrium has been also described by the UV-vis absorbance study which yielded the reaction enthalpy ( $\Delta H^\circ = 9.5 \text{ kJ mol}^{-1}$ ) and the reaction entropy ( $\Delta S^\circ = 33 \text{ J mol}^{-1}\text{K}^{-1}$ ). We assume that the same hydration equilibrium, characterized by these thermodynamic parameters, exists for [Gd(bp12c4)(H<sub>2</sub>O)<sub>q</sub>]<sup>+</sup> as well. The reduced <sup>17</sup>O relaxation rates and chemical shifts have been therefore obtained from the experimental relaxation rates and chemical shifts by taking into account the temperature dependency of the hydration equilibrium, which allows calculating the average  $q$  value at each temperature. The data are presented in Figure 5.

The <sup>17</sup>O reduced transverse relaxation rates ( $1/T_{2r}$ ) decrease with increasing temperature in the whole temperature range investigated, indicating that they are in the

(43) Margerum, D. W.; Zabin, B. A.; Janes, D. L. *Inorg. Chem.* **1966**, *5*, 250.

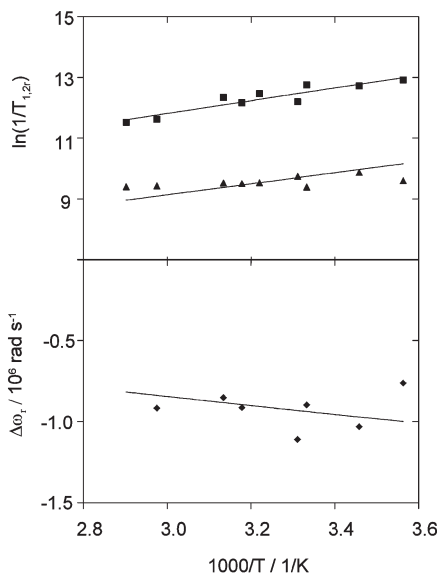


**Figure 5.** Reduced longitudinal ( $\blacktriangle$ ) and transverse ( $\blacksquare$ )  $^{17}\text{O}$  NMR relaxation rates and  $^{17}\text{O}$  NMR chemical shifts ( $\blacklozenge$ ) of a  $[\text{Gd}(\text{bp}12\text{c}4)\text{-(H}_2\text{O)}_4]^+$  solution at 11.75 T and pH = 6. The lines represent the best fit of the data as explained in the text.

fast exchange region. Here the reduced transverse relaxation rate is defined by the transverse relaxation rate of the bound water oxygen,  $1/T_{2m}$ , which is in turn influenced by the water exchange rate,  $k_{\text{ex}}$ , the longitudinal electronic relaxation rate,  $1/T_{1e}$ , and the scalar coupling constant,  $A/\hbar$ . The reduced  $^{17}\text{O}$  chemical shifts are determined by  $A/\hbar$ . Transverse  $^{17}\text{O}$  relaxation is governed by the scalar relaxation mechanism and thus contains no information on the rotational motion of the system. In contrast to  $1/T_{2r}$ , the longitudinal  $^{17}\text{O}$  relaxation rates,  $1/T_{1r}$ , are determined by dipole–dipole and quadrupolar relaxation mechanisms, both related to rotation. The dipolar term depends on the  $\text{Gd}^{3+}$ –water oxygen distance,  $r_{\text{GdO}}$ , while the quadrupolar term is influenced by the quadrupolar coupling constant,  $\chi(1 + \eta^2/3)^{1/2}$ . The experimental data have been fitted to the Solomon–Bloembergen–Morgan theory of paramagnetic relaxation using the equations presented in the Supporting Information. In the fitting procedure,  $r_{\text{GdO}}$  has been fixed to 2.50 Å, based on available crystal structures,<sup>44,45</sup> and recent ENDOR results.<sup>46</sup> The quadrupolar coupling constant,  $\chi(1 + \eta^2/3)^{1/2}$ , has been set to the value for pure water, 7.58 MHz. We should note that a  $r_{\text{GdO}}$  value of 2.585 Å was obtained for  $[\text{Gd}(\text{bp}12\text{c}4)(\text{H}_2\text{O})]^+$  from DFT calculations performed in vacuo.<sup>15</sup> However, a shorter distance is expected in aqueous solution, where a stronger water ion interaction arises from solvent polarization effects that increase the dipole moment of the free water molecules.<sup>47</sup> The empirical constant describing the outer sphere contribution to the  $^{17}\text{O}$  chemical shift,  $C_{\text{os}}$ , was fixed to 0. The electron spin relaxation rate,  $1/T_{1e}$ , has been fitted to a simple exponential function. The following parameters have

been adjusted: the water exchange rate,  $k_{\text{ex}}^{298}$ , or the activation entropy,  $\Delta S^\ddagger$ , the activation enthalpy for water exchange,  $\Delta H^\ddagger$ , the scalar coupling constant,  $A/\hbar$ , the rotational correlation time ( $\tau_{\text{R}}^{298}$ ) and its activation energy,  $E_{\text{R}}$ , and the electron spin relaxation rate at 298 K,  $1/T_{1e}^{298}$  and its activation energy,  $E_{\text{T}}$ . The values obtained for these parameters are presented in Table 3. For  $1/T_{1e}^{298}$ , we calculated  $(1.9 \pm 0.4) \times 10^7 \text{ s}^{-1}$ , while  $E_{\text{T}}$  was fixed to 1 kJ/mol, otherwise small negative values were obtained.

The water exchange rate is very high on  $[\text{Gd}(\text{bp}12\text{c}4)\text{-(H}_2\text{O)}_4]^+$ , being within the same order of magnitude as for the  $[\text{Gd}(\text{H}_2\text{O})_8]^{3+}$  aqua ion or for the previously studied  $[\text{Gd}(\text{L}^2)]^{3+}$  complex (Chart 1). To the best of our knowledge, this is the fastest water exchange on a macrocyclic  $\text{Gd}^{3+}$  complex ever reported. In the fast exchange regime, the  $^{17}\text{O}$  transverse relaxation rates are influenced by both the water exchange and the electron spin relaxation. We should note that the electron spin relaxation,  $1/T_{1e}$ , has a very limited contribution, representing maximum 10% in the correlation time  $\tau_{\text{c}}$  governing the relaxation rate of the bound water oxygen,  $1/T_{2m}$  ( $1/\tau_{\text{c}} = k_{\text{ex}} + 1/T_{1e}$ ). Therefore, the water exchange rate can be obtained with a very good certitude.

The activation entropy is strongly negative, indicating that the water exchange process has an associative character, that is, the incoming water enters the inner coordination sphere of the complex before the departure of the leaving water molecule. So far, few  $\text{Gd}^{3+}$  complexes have been reported to have associative water exchange,<sup>48–51</sup> all of them are octa-coordinate. Most  $\text{Gd}^{3+}$  complexes studied with respect to their water exchange, poly(aminocarboxylates) in majority, were nine-coordinate and presented dissociatively activated water exchange. This could be related to the nature of  $\text{Gd}^{3+}$  that prefers the typical coordination numbers 8 or 9 in solution. Consequently, the water exchange of octa-coordinate complexes will proceed via an associatively activated mechanism, involving a nine-coordinate transition state, while that of the nine-coordinate complexes will go through an eight-coordinate transition state in a dissociatively activated process. As a general rule, the water exchange rate is higher for associatively activated processes. In our case, the hydration equilibrium is between a nine-coordinate, monohydrated, and a ten-coordinate, bishydrated species, present in comparable quantities. Given the large negative value obtained for the activation entropy, one could speculate that the water exchange on the nine-coordinate species, which can be expected to proceed via an associative pathway, is mainly responsible for the observed  $^{17}\text{O}$   $T_2$  effect, while the contribution of the ten-coordinate, bishydrated species, which should proceed via a dissociative mechanism, would be negligible. The positive charge of the complex could be another

(44) Spirlet, M.-R.; Rebizant, J.; Desreux, J. F.; Loncin, M.-F. *Inorg. Chem.* **1984**, *23*, 359–363.

(45) Stezowski, J. J.; Hoard, J. L. *Isr. J. Chem.* **1984**, *24*, 323–334.

(46) Raitisimring, A. M.; Astashkin, A. V.; Baute, D.; Goldfarb, D.; Caravan, P. *J. Phys. Chem. A* **2004**, *108*, 7318–7323.

(47) Djanashvili, K.; Platas-Iglesias, C.; Peters, J. A. *Dalton Trans.* **2008**, 602–607.

(48) Powell, H. D.; Ni Dhubbghaill, O. M.; Pubanz, D.; Helm, L.; Lebedev, Y.; Schlaepfer, W.; Merbach, A. E. *J. Am. Chem. Soc.* **1996**, *118*, 9333–9346.

(49) Toth, E.; Helm, L.; Merbach, A. E.; Hedinger, R.; Hegetschweiler, K.; Jánossy, A. *Inorg. Chem.* **1998**, *37*, 4104–4113.

(50) Thompson, M. K.; Botta, M.; Nicolle, G. M.; Helm, L.; Aime, S.; Merbach, A. E.; Raymond, K. N. *J. Am. Chem. Soc.* **2003**, *125*, 14274–14275.

(51) Burai, L.; Toth, E.; Bazin, H.; Benmelouka, M.; Jaszberenyi, Z.; Helm, L.; Merbach, A. E. *Dalton Trans.* **2006**, 629–634.



**Table 3.** Parameters Obtained from the Fitting of the  $^{17}\text{O}$  NMR Relaxation Rates and Chemical Shifts at 11.7 T

	$[\text{Gd}(\text{bp}12\text{c}4)(\text{H}_2\text{O})_q]^+$	$[\text{Gd}(\text{DTPA})(\text{H}_2\text{O})]^{2-a}$	$[\text{Gd}(\text{H}_2\text{O})_8]^{3+a}$	$[\text{Gd}(\text{L}^2)]^{3-b}$
$k_{\text{ex}}/10^6 \text{ s}^{-1}$	$220 \pm 15$	3.3	800	700
$\Delta H^\ddagger/\text{kJ mol}^{-1}$	$14.8 \pm 3.0$	51.6	15.3	22
$\Delta S^\ddagger/\text{J mol}^{-1} \text{ K}^{-1}$	$-35 \pm 8$	+56	-23	-3
$A/\hbar/10^6 \text{ rad s}^{-1}$	$-3.4 \pm 0.3$	-3.8	-5.3	-3.5
$\tau_{\text{R}}/ps$	$105 \pm 16$	103	41	155
$E_{\text{R}}/\text{kJ mol}^{-1}$	$15.0 \pm 4.2$	17.3	15	27

<sup>a</sup> Ref 48. <sup>b</sup> Ref 9b.

factor that contributes to the associatively activated process. The approach of the second water molecule with its oxygen bearing a partial negative charge should be favored by a positive charge on the complex. Consequently, the water exchange on the bishydrated complex should be considerably slower than that on the monohydrated one, in accordance with the general observation that associative exchanges are faster than dissociative ones. On the basis of this reasoning, we tried to fit the  $1/T_{2r}$  values by assuming that the only species that contributes to the water exchange is the monohydrated complex. By taking into account the temperature-dependent variation of its ratio (based on the UV-vis study on the  $\text{Eu}^{3+}$  analogue), we obtained  $k_{\text{ex}}^{298} = (8.0 \pm 1.0) \times 10^8 \text{ s}^{-1}$  for  $[\text{Gd}(\text{bp}12\text{c}4)(\text{H}_2\text{O})]^+$  ( $\Delta H^\ddagger = 18.7 \text{ kJ/mol}$ ). However, we do not possess any tool to decide whether the nine-coordinate species is the only contributor to the reduced  $^{17}\text{O}$  transverse relaxation rates. Therefore, we prefer to report the effective  $k_{\text{ex}}$  value as shown in Table 3. In any case, if we consider practical applications of this complex as an MRI contrast agent, it is the effective  $k_{\text{ex}}$  value that will determine the efficiency of the chelate in enhancing water proton relaxation.

The very fast exchange observed for  $[\text{Gd}(\text{bp}12\text{c}4)(\text{H}_2\text{O})_q]^+$  is likely related to the hydration equilibrium of the complex, and more importantly, to the very flexible inner coordination sphere around the metal ion. Other  $\text{Gd}^{3+}$  complexes which also present hydration equilibrium do not necessarily have such extreme water exchange rates. For instance,  $[\text{Gd}(\text{DO}3\text{A})(\text{H}_2\text{O})_q]$  and  $[\text{Gd}(\text{DO}2\text{A})(\text{H}_2\text{O})_q]^+$  both have differently hydrated species in aqueous solution ( $q_{\text{ave}} = 1.8$  and  $2.8$ , respectively), but they show only a limited increase of the water exchange rate as compared to the monohydrated  $[\text{Gd}(\text{DOTA})(\text{H}_2\text{O})]^-$ .<sup>52</sup> For these macrocyclic complexes, the most important factor that limits water exchange is probably the rigidity of the inner sphere.

Concerning the other parameters calculated in the fit, the rotational correlation time has a reasonable value for a small molecular weight complex. For the scalar coupling constant,  $A/\hbar$ , we obtained  $-(3.4 \pm 0.3) \times 10^6 \text{ rad s}^{-1}$ , which is in good accordance with values reported for  $\text{Gd}^{3+}$  complexes.<sup>48</sup> This also confirms that the hydration number used in the calculations is correct. We should also note that the slope of the curve of the reduced chemical shifts versus inverse temperature is nicely reproduced by the fit, which supports that the parameters characterizing the temperature dependency of the hydration equilibrium are correct (Figure 5).

**Anion Binding Studies.** Coordinatively unsaturated lanthanide complexes containing two inner-sphere water molecules, such as  $\text{Ln}^{3+}$  DO3A-like complexes, are known to bind biologically relevant anions such as hydrogencarbonate, phosphate, or citrate.<sup>53</sup> The ability of these lanthanide complexes to form ternary complexes with anions is likely related to the presence of the two inner-sphere water molecules coordinated to the  $\text{Ln}^{3+}$  ion in adjacent positions. Indeed, several coordinatively unsaturated  $q = 2$  lanthanide complexes either do not bind anions or the observed binding is very weak.<sup>54</sup> Most likely this is due to an unfavorable, non adjacent location of the inner-sphere water molecules around the metal ion. In a previous study on the solution structure of  $[\text{Ln}(\text{bp}12\text{c}4)(\text{H}_2\text{O})_q]^+$  complexes, we have shown that in  $q = 2$  complexes the two inner-sphere water molecules occupy adjacent positions in the metal ion coordination sphere.<sup>15</sup> Thus, these  $\text{Ln}^{3+}$  complexes of  $\text{bp}12\text{c}4^{2-}$  are expected to bind anions in aqueous solution. The formation of ternary complexes between  $[\text{Gd}(\text{bp}12\text{c}4)(\text{H}_2\text{O})_q]^+$  and hydrogencarbonate, phosphate, and citrate ions has been studied by measuring the longitudinal relaxation rates ( $1/T_1$ ) of water protons at 500 MHz and 25 °C (pH = 7.4, 0.01 M HEPES,  $I = 0.15 \text{ M NaCl}$ ). The concentration of the  $\text{Gd}^{3+}$ -complex was  $\sim 1 \text{ mM}$  while the concentration of each anion varied between 0 and 36 mM. Anion addition caused a decrease in relaxivity, in agreement with the replacement of inner-sphere water molecules by the anion (for citrate see Figure 6, curves for hydrogencarbonate and phosphate are shown in the Supporting Information). Plots of the relaxivity versus the  $[\text{anion}]/[\text{complex}]$  ratio show saturation profiles for all investigated anions. The least-squares fitting of the titration profiles allowed us to determine the binding constants listed in Table 4. The fitting of the experimental data also provides the relaxivity of the ternary complexes ( $r_{1,t}$ , Table 4).  $[\text{Gd}(\text{bp}12\text{c}4)(\text{H}_2\text{O})_q]^+$  binds the three investigated anions rather strongly, as expected for a positively charged complex, with binding constants ranging between about 250 and 630  $\text{M}^{-1}$ , in the following binding trend: hydrogencarbonate > phosphate  $\approx$  citrate. The relaxivities calculated for the three ternary complexes are very similar and consistent with  $q = 0$ .

In bovine serum, the relaxivity of  $[\text{Gd}(\text{bp}12\text{c}4)(\text{H}_2\text{O})_q]^+$  is slightly diminished ( $r_1 = 3.19 \text{ mM}^{-1} \text{ s}^{-1}$  vs  $3.89 \text{ mM}^{-1} \text{ s}^{-1}$  in

(52) Toth, E.; Ni Dhubhghaill, O. M.; Besson, G.; Helm, L.; Merbach, A. E. *Magn. Reson. Chem.* **1999**, *37*, 701–708.

(53) (a) Aime, S.; Botta, M.; Bruce, J. I.; Mainero, V.; Parker, D.; Terreno, E. *Chem. Commun.* **2001**, 115–116. (b) Bruce, J. I.; Dickins, R. S.; Govenlock, L. J.; Gunnlaugsson, T.; Lopinski, S.; Lowe, M. P.; Parker, D.; Peacock, R. D.; Perry, J. J. B.; Aime, S.; Botta, M. *J. Am. Chem. Soc.* **2000**, *122*, 9674–9684.

(54) Loureiro de Sousa, P.; Livramento, J. B.; Helm, L.; Merbach, A. E.; Meme, W.; Doan, B.-T.; Beloeil, J.-C.; Prata, M. I. M.; Santos, A. C.; Geraldes, C. F. G. C.; Toth, E. *Contrast Media Mol. Imaging* **2008**, *3*, 78–85.

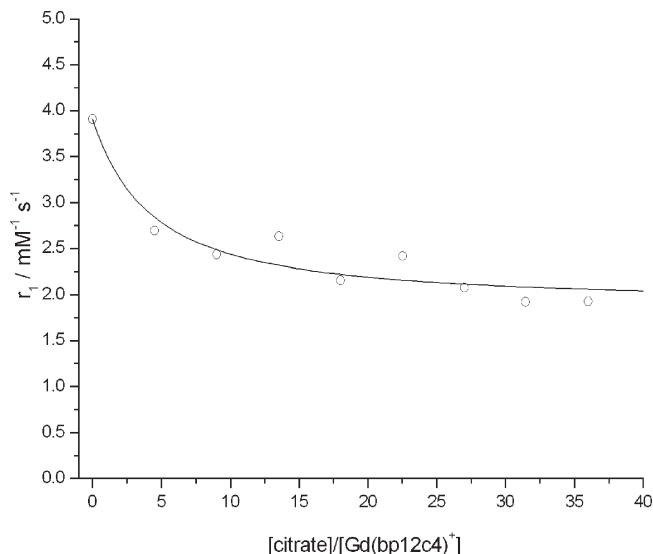


**Figure 6.** Relaxivity of  $[\text{Gd}(\text{bp}12\text{c}4)(\text{H}_2\text{O})_q]^{3+}$  ( $\sim 1$  mM) in the presence of increasing citrate concentration, at 500 MHz and 25 °C. The line is the fitted curve as explained in the text.

**Table 4.** Binding Constants ( $K_{\text{aff}}$ ,  $\text{M}^{-1}$ ) for the Interaction of  $[\text{Gd}(\text{bp}12\text{c}4)(\text{H}_2\text{O})_q]^{3+}$  with Different Anions and Relaxivity ( $r_{1,t}$ ,  $\text{mM}^{-1} \text{s}^{-1}$ ) of the Ternary Complex Obtained from the Fit of the Relaxivity Measurements at 25 °C<sup>a</sup>

	citrate	$\text{HCO}_3^-$	phosphate
$K_{\text{aff}}$	$280 \pm 20$	$630 \pm 50$	$250 \pm 20$
$r_{1,t}$	$1.90 \pm 0.02$	$2.15 \pm 0.02$	$1.90 \pm 0.03$

<sup>a</sup> pH = 7.4, 0.01 M HEPES,  $I = 0.15$  M NaCl.

pure water, 25 °C, 500 MHz), reflecting the partial replacement of the inner sphere water.

The binding of hydrogencarbonate and citrate to the  $\text{Eu}^{3+}$  complex of  $\text{bp}12\text{c}4^{2-}$  was also investigated by observing the changes in the emission intensity and lifetime of the metal centered emission. The emission spectrum of a  $10^{-5}$  M solution of the  $\text{Eu}^{3+}$  complex in  $\text{H}_2\text{O}$  [pH 7.4 (0.01 M HEPES), 0.15 M NaCl], obtained under excitation through the ligand bands at 272 nm displays the typical  ${}^5\text{D}_0 \rightarrow {}^7\text{F}_J$  transitions (Figure 7,  $J = 0-4$ ). The emission lifetime of the  $\text{Eu}({}^5\text{D}_0)$  excited level determined under these conditions amounts to 0.50 ms, a value that is nearly identical to that determined previously in unbuffered solution at pH 8 and in the absence of NaCl (0.52 ms).<sup>15</sup> Addition of hydrogencarbonate provokes important changes in the emission spectrum of the complex (Figure 7). In particular, anion addition causes an important increase of the intensity of the hypersensitive and electric-dipole allowed  ${}^5\text{D}_0 \rightarrow {}^7\text{F}_2$  transition, while the intensity of the remaining  ${}^5\text{D}_0 \rightarrow {}^7\text{F}_J$  transitions increases to a lesser extent. It has been demonstrated that the nature and polarizability of the group occupying a position on or close to the principal axis of the complex affects the relative intensity of the  ${}^5\text{D}_0 \rightarrow {}^7\text{F}_2$  transition.<sup>55</sup> The more polarizable the axial donor atom is, the greater the relative intensity of the  ${}^5\text{D}_0 \rightarrow {}^7\text{F}_2$  emission band. In a previous paper, we have demonstrated the principal

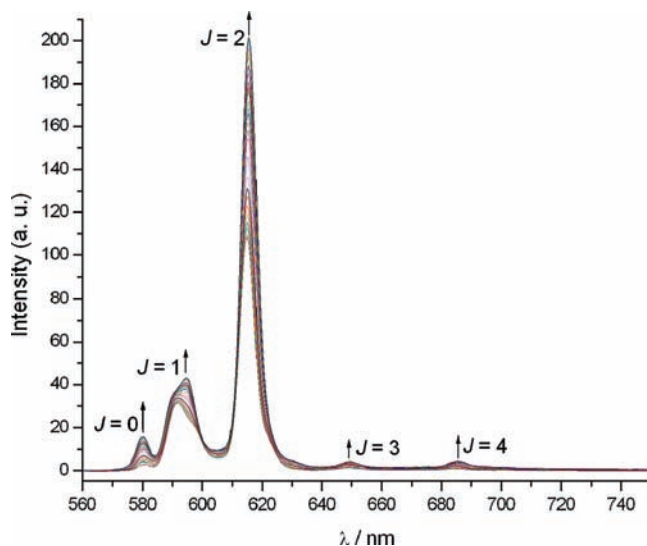


**Figure 7.** Variation of the emission spectrum for  $[\text{Eu}(\text{bp}12\text{c}4)(\text{H}_2\text{O})_q]^{3+}$  following addition of hydrogencarbonate [pH = 7.4 (HEPES), [complex] = ca.  $10^{-5}$  M,  $\lambda_{\text{exc}} = 272$  nm,  $I = 0.15$  M NaCl].

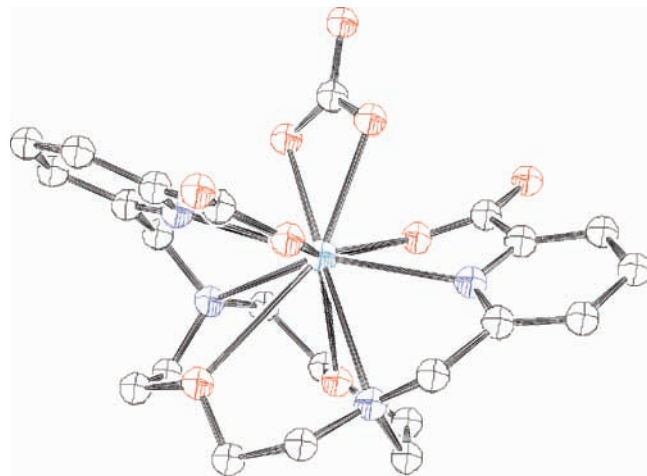


**Figure 8.** Calculated minimum energy conformation of the  $[\text{Gd}(\text{bp}12\text{c}4)]^+ \cdot \text{HCO}_3^-$  ternary complex as optimized in vacuo at the B3LYP/6-31G(d) level. Hydrogen atoms are omitted for simplicity.

magnetic axis of the  $\text{Yb}^{3+}$  complex is coincident with the  $\text{C}_2$  symmetry axis of the molecule, which is perpendicular to the best plane defined by the donor atoms of the macrocycle and contains the lanthanide ion. In the case of the  $q = 1$  complexes, the oxygen atom of the inner-sphere water molecule is on the principal axis. Thus, the increase of the relative intensity of the  ${}^5\text{D}_0 \rightarrow {}^7\text{F}_2$  transition is attributed to the substitution of hard coordinated water molecules by more polarizable C–O donors of the anion. The spectra shown in Figure 7 also evidence substantial changes in the splitting of the  ${}^5\text{D}_0 \rightarrow {}^7\text{F}_1$  manifold upon anion addition. The splitting of the  $J = 1$  manifold is related to the magnitude of the second order crystal field coefficient, which in turns depends on the polarizability of the donor atoms placed close to the principal axis of the complex.<sup>56</sup> Citrate binding provokes similar spectral

(55) (a) Dickins, R. S.; Parker, D.; Bruce, J. I.; Tozer, D. J. *Dalton Trans.* **2003**, 1264–1271. (b) Murray, B. S.; New, E. J.; Pal, R.; Parker, D. *Org. Biomol. Chem.* **2008**, *6*, 2085–2094. (c) Bretonniere, Y.; Cann, M. J.; Parker, D.; Slater, R. *Org. Biomol. Chem.* **2004**, *2*, 1624–1632.

(56) Dickins, R. S.; Aime, S.; Batsanov, A. S.; Beeby, A.; Botta, M.; Bruce, J. I.; Howard, J. A. K.; Love, C. S.; Parker, D.; Peacock, R. D.; Puschmann J. *Am. Chem. Soc.* **2002**, *124*, 12697–12705.

**Table 5.** Values of the Bond Distances of the Gd<sup>3+</sup> Coordination Environment of the Minimum Energy Conformations Calculated for [Gd(bp12c4)(H<sub>2</sub>O)<sub>2</sub>]<sup>+</sup>, [Gd(bp12c4)(HCO<sub>3</sub>)], and [Gd(bp12c4)(H<sub>2</sub>PO<sub>4</sub>)] Complexes at the B3LYP/6-31G(d) Level<sup>a</sup>

	[Gd(bp12c4)(H <sub>2</sub> O) <sub>2</sub> ] <sup>+b</sup>	[Gd(bp12c4)(HCO <sub>3</sub> )]	[Gd(bp12c4)(H <sub>2</sub> PO <sub>4</sub> )]
Gd–N <sub>PY</sub>	2.565	2.549	2.540
	2.646	2.611	2.666
Gd–O <sub>C</sub>	2.684	3.038	3.200
	2.520	2.578	2.563
Gd–O <sub>COO</sub>	2.351	2.334	2.313
	2.388	2.422	2.494
Gd–N <sub>AM</sub>	2.723	2.794	2.848
	2.806	2.915	2.986
Gd–O <sub>A</sub>		2.513	2.511
		2.442	2.406

<sup>a</sup> Distances (Å), angles (deg.). N<sub>AM</sub> = amine nitrogen atoms; N<sub>PY</sub> = pyridyl nitrogen atoms; O<sub>COO</sub> = carboxylate oxygen atoms; O<sub>C</sub> = crown oxygen atoms; O<sub>A</sub> = oxyanion oxygen atom. <sup>b</sup> Ref 15.

changes in the emission spectrum of the Eu<sup>3+</sup> complex (Figure S2, Supporting Information).

The formation of the ternary adduct results in a longer emission lifetime of the Eu(<sup>5</sup>D<sub>0</sub>) excited level. The emission lifetime determined upon addition of 590 equiv of citrate amounts to 0.93 ms. This value is substantially longer than that obtained in the absence of anion (0.50 ms) considering that under these condition the concentration of the ternary adduct is expected to be about 62%. These results are in agreement with the formation of ternary adducts in which inner-sphere water molecules are replaced by anion binding.

To obtain information about the structure of the ternary complexes, the [Gd(bp12c4)(HCO<sub>3</sub>)] and [Gd(bp12c4)(H<sub>2</sub>PO<sub>4</sub>)] systems were investigated by DFT calculations (B3LYP model). The effective core potential (ECP) of Dolg et al. and the related [5s4p3d]-GTO valence basis set was applied in these calculations.<sup>28</sup> This ECP includes 46 + 4f<sup>7</sup> electrons in the core, leaving the outermost 11 electrons to be treated explicitly, and it has been demonstrated to provide reliable results for several lanthanide complexes with both macrocyclic<sup>57,58</sup> or acyclic<sup>59</sup> ligands. We have previously shown that the complexes of bp12c4<sup>2-</sup> present two sources of helicity: one associated with the layout of the picolate pendant arms (absolute configuration Δ or Λ), and the other to the four five-membered chelate rings formed by the binding of the crown moiety (each of them showing absolute configuration δ or λ).<sup>15</sup> Since enantiomers have the same physicochemical properties in a non-chiral environment we have only considered four diastereoisomeric forms of the complexes in our conformational analysis: Λ(λλλλ), Δ(λλλλ), Λ(δλδλ), and Λ(λδλδ). Previous theoretical calculations performed at the DFT (B3LYP) level evidence that the change in hydration number across the lanthanide series is accompanied by a change in the conformation that the complexes adopt in solution [Δ(λλλλ) for *q* = 2 and Λ(δλδλ) for *q* = 1]. Our calculations on [Gd(bp12c4)(HCO<sub>3</sub>)] and [Gd(bp12c4)(H<sub>2</sub>PO<sub>4</sub>)] predict the Δ(λλλλ) conformation to be the most stable for both ternary complexes. This is attributed to the fact that the Δ(λλλλ) conformation possesses a more open structure than

the Λ(δλδλ) one, which is the most stable one in the case of *q* = 1 complexes.<sup>15</sup> The optimized geometry for the complex with hydrogencarbonate is shown in Figure 8.

Our calculations predict a slightly asymmetrical binding of both hydrogencarbonate and dihydrogenphosphate to the Gd<sup>3+</sup> ion, the Gd<sup>3+</sup>–O<sub>anion</sub> distances amounting to 2.44 and 2.51 Å (HCO<sub>3</sub><sup>-</sup>) and 2.41 and 2.51 Å (H<sub>2</sub>PO<sub>4</sub><sup>-</sup>). Anion coordination also results in pronounced changes in the bond distances of the Gd<sup>3+</sup> coordination environment in comparison to [Gd(bp12c4)(H<sub>2</sub>O)<sub>2</sub>]<sup>+</sup> (Table 5). It provokes an important lengthening of the distance to one of the oxygen atoms of the crown moiety (by 0.36 and 0.56 Å for carbonate and phosphate, respectively). The distance between Gd<sup>3+</sup> and one of the amine nitrogen atoms also increases substantially upon carbonate or phosphate binding (by 0.10 and 0.18 Å, respectively). In overall, the phosphate coordination induces a more important distortion of the metal coordination environment than carbonate coordination, in line with the higher binding constant. This is explained with a more important steric hindrance around the pendant arms of the ligand caused by the coordination of a tetrahedral anion such as phosphate compared to the planar carbonate. The concentration of HPO<sub>4</sub><sup>2-</sup> in solution at pH 7.4 is very similar to that of H<sub>2</sub>PO<sub>4</sub><sup>-</sup>. Thus, we also investigated the coordination of HPO<sub>4</sub><sup>2-</sup> by performing calculations on the [Gd(bp12c4)(HPO<sub>4</sub>)]<sup>-</sup> system. Our results confirm that the coordination of phosphate induces a more important distortion of the metal coordination environment than the coordination of carbonate (see the Supporting Information).

## Conclusions

The stability constants of the [Ln(bp12c4)]<sup>+</sup> complexes have been obtained from direct potentiometric titrations, as the complex formation is fast. The stability increases from the early lanthanides to the middle of the series, then remains relatively constant or slightly declines for the heavier lanthanides, similarly to Ln<sup>3+</sup>-DTPA chelates. In the presence of Zn<sup>2+</sup>, the dissociation of [Gd(bp12c4)]<sup>+</sup> proceeds both via proton- and metal-assisted pathways, and in this respect, this system is intermediate between DTPA-type and macrocyclic chelates, for which the dissociation is predominated by metal- or proton-assisted pathways, respectively. The Cu<sup>2+</sup> exchange shows an unexpected pH dependency, with the observed rate constants decreasing with increasing proton concentration.

(57) Gonzalez-Lorenzo, M.; Platas-Iglesias, C.; Avecilla, F.; Faulkner, S.; Pope, S. J. A.; de Blas, A.; Rodriguez-Blas, T. *Inorg. Chem.* **2005**, *44*, 4254–4262.

(58) Cosentino, U.; Villa, A.; Pitea, D.; Moro, G.; Barone, V.; Maiocchi, A. *J. Am. Chem. Soc.* **2002**, *124*, 4901–4909.

(59) Ouali, N.; Bocquet, B.; Rigault, S.; Morgantini, P.-Y.; Weber, J.; Piguet, C. *Inorg. Chem.* **2002**, *41*, 1436–1445.

The  $[\text{Gd}(\text{bp}12\text{c}4)(\text{H}_2\text{O})_q]^+$  complex is present in hydration equilibrium between nine-coordinate, monohydrated, and ten-coordinate, bishydrated species. The rate of water exchange as assessed by  $^{17}\text{O}$  NMR is extremely high, close to that of the  $\text{Gd}^{3+}$  aqua ion itself. This fast exchange can be accounted for by the flexible nature of the inner coordination sphere. The activation entropy suggests a strong associative character for the water exchange which presumably involves only the nine-coordinate, monohydrated species. Relaxometric and luminescence measurements, together with DFT calculations, indicate strong anion binding to  $[\text{Ln}(\text{bp}12\text{c}4)(\text{H}_2\text{O})_q]^+$  complexes, consistent with the complete replacement of the inner sphere water molecules.

**Acknowledgment.** A.R.-S., M.M.-I., D.E.-G., C.P.-I., A.de B. and T.R.-B. thank the Ministerio de Educación y Ciencia and FEDER (CTQ2006-07875/PPQ) and Xunta

de Galicia (INCITE08ENA103005ES) for financial support. Z.P. acknowledges the grant of the RFR program of the French Ministry of Education and Research. This research was performed in the framework of the EU COST Action D38 “Metal-Based Systems for Molecular Imaging Applications”. The authors are indebted to Centro de Supercomputación de Galicia for providing the computer facilities.

**Supporting Information Available:** Changes in the relaxivity of the  $\text{Gd}^{3+}$  complex of  $\text{bp}12\text{c}4^{2-}$  upon addition of anions (Figure S1), changes in the emission spectrum of the  $\text{Eu}^{3+}$  complex of  $\text{bp}12\text{c}4^{2-}$  upon citrate binding (Figure S2), UV–vis spectra of the system  $\text{Gdbp}12\text{c}4^+-\text{Cu}^{2+}$  (Figure S3), set of equation used for the analysis of the  $^{17}\text{O}$  NMR data and DFT optimized Cartesian coordinates (Å) for the  $[\text{Gd}(\text{bp}12\text{c}4)]^+\cdot\text{HCO}_3^-$ ,  $[\text{Gd}(\text{bp}12\text{c}4)]^+\cdot\text{H}_2\text{PO}_4^-$ , and  $[\text{Gd}(\text{bp}12\text{c}4)]^+\cdot\text{HPO}_4^{2-}$  systems. This material is available free of charge via the Internet at <http://pubs.acs.org>.